Model-Independent Calculation of Radiative Neutron Capture on Lithium-7

Gautam Rupak[1,*] and Renato Higa[2,†]

[1]Department of Physics and Astronomy and High Performance Computing Collaboratory, Mississippi State University, Mississippi State, Mississippi 39762, USA

[2]Kernfysisch Versneller Instituut, Theory Group, University of Groningen, 9747AA Groningen, The Netherlands

(Received 26 January 2011; published 31 May 2011)

The radiative neutron capture on lithium-7 is calculated model independently using a low-energy halo effective field theory. The cross section is expressed in terms of scattering parameters directly related to the S-matrix elements. It depends on the poorly known p-wave effective range parameter r_1. This constitutes the largest uncertainty in traditional model calculations. It is explicitly demonstrated by comparing with potential model calculations. A single parameter fit describes the low-energy data extremely well and yields $r_1 \approx -1.47$ fm^{-1}.

DOI: 10.1103/PhysRevLett.106.222501 PACS numbers: 25.40.Lw, 25.20.−x

Introduction.—Low-energy nuclear reactions play a crucial role in big bang nucleosynthesis (BBN), stellar burning, and element synthesis at supernova sites [1–3]. They also play an important role in testing astrophysical models and physics beyond the standard model (SM) of particle physics. Often the key nuclear reactions occur at energies that are not directly accessible in terrestrial laboratories. Radiative proton capture on beryllium ^{7}Be$(p,\gamma)^8$B is one of them—it is important for boron-8 production in the Sun, whose weak decay results in the high energy neutrinos that are detected at terrestrial laboratories looking for physics beyond the SM. The relevant solar energy, the Gamow peak, for this reaction is around 20 keV [4]. This necessitates theoretical extrapolation to solar energies of known experimental capture data from above around 100 keV. Current extrapolations introduce 5%–20% error [4–6]. A model-independent effective field theory (EFT) calculation would be very useful in constraining them.

In an EFT, one identifies the relevant low-energy degrees of freedom and constructs the most general interactions allowed by symmetry without modeling the short distance physics. The interactions are organized in a low momentum expansion. At a given order in the expansion, a finite number of interactions has to be considered and an *a priori* estimate of the theoretical error can be made. The latter is crucial due to astrophysical demands [1,2,4]. The former is important because many processes involve external currents, and any prescription used in phenomenological models involves some uncertainty. As an example, the cross section for $n(p,\gamma)d$ at BBN energies was calculated within EFT to an accuracy of about 1% [7]. Systematic treatment of two-body currents was necessary to achieve this level of precision, and it addressed a critical need [1] for nuclear theory input in astrophysics.

Applications of EFT to systems with $A \gtrsim 5$ is still challenging. However, some loosely bound systems, such as halo nuclei, open new possibilities. The small separation energy of the valence nucleons in halo nuclei provides a small expansion parameter for constructing a halo EFT [8]. The ^{8}B is a halo nucleus with a proton weakly bound to the ^{7}Be core by 0.1375 MeV. The ^{7}Be$(p,\gamma)^8$B calculation would be an important step in developing EFT techniques for weakly bound nuclei as has been accomplished in the few nucleon systems. In Ref. [9], electromagnetic transition in the halo system ^{11}Be was considered. Experiments such as those planned at the future FRIB [10] would explore exotic nuclei near the drip lines where halo systems abound. Structure and reactions with halo EFT can serve as benchmarks for phenomenological models.

We consider the low-energy reaction ^{7}Li$(n,\gamma)^8$Li, which is an isospin mirror to ^{7}Be$(p,\gamma)^8$B. The n-^{7}Li system allows formulating the EFT for the nuclear interactions without the added complication of the Coulomb force. Additionally, ^{7}Li$(n,\gamma)^8$Li is a key process in inhomogeneous BBN models. Its reaction rate impacts the abundance of ^{7}Li and the production of carbon-oxygen-nitrogen in the early universe, thus constraining alternative astrophysical scenarios [11]. Traditionally ^{7}Li$(n,\gamma)^8$Li has been calculated in a single-particle approximation as a ^{7}Li core plus a valence neutron interacting via a Woods-Saxon potential, e.g., Refs. [5,12,13]. This approximation is valid at low energies where the internal structure of the ^{7}Li core is not probed, for example, much below the threshold for ^{7}Li$(\gamma,{}^3\mathrm{He})\alpha$, which is around 2.5 MeV. In the following we show that the capture cross section below $\sim$100 keV is very sensitive to the p-wave effective range r_1, a result that carries over to the mirror ^{7}Be$(p,\gamma)^8$B reaction.

Interaction.—The relevant low-energy nuclear degrees of freedom, here, are the pointlike neutron, ^{7}Li, and ^{8}Li with spin-parity $\frac{1}{2}^+$, $\frac{3}{2}^-$, and 2^+, respectively. The relevant incoming n-^{7}Li states are s waves: $^3S_1$, $^5S_2$ in the spectroscopic notation $^{2S+1}L_J$. The ground state is a 2^+ state that is primarily the symmetric combination of the possible p-wave states $^3P_2$ and $^5P_2$ [14]. Conservation of parity

implies that the reaction $^7\mathrm{Li}(n,\gamma)^8\mathrm{Li}$ proceeds through the electric dipole transition $E1$ at lowest order.

The leading order (LO) s-wave interactions contain no derivatives. The two-component spin-$\frac{1}{2}$ neutron field $N(x)$ and four-component spin-$\frac{3}{2}$ ^{7}Li field $C(x)$ can be combined into the $^3S_1$ and $^5S_2$ states using the Clebsch-Gordan coefficient matrices F_i, Q_{ij} as $N^T F_i C$ and $N^T Q_{ij} C$, respectively. The vector index in F_i relates to the three magnetic quantum numbers in the spin $S=1$ channel. The symmetric, traceless matrices Q_{ij} relate to the five magnetic quantum numbers in the spin $S=2$ channel. We write the s-wave LO Lagrangian as

$$\mathcal{L}^{(s)} = g^{(1)}(N^T F_i C)^\dagger (N^T F_i C) + g^{(2)}(N^T Q_{ij} C)^\dagger (N^T Q_{ij} C), \quad (1)$$

where a single momentum-independent interaction in each of the $^3S_1$ and $^5S_2$ channels was kept. The higher derivative terms are suppressed at low energy. The 2×4 Clebsch-Gordan matrices are given as

$$F_i = -\frac{i\sqrt{3}}{2}\sigma_2 S_i, \quad Q_{ij} = -\frac{i}{\sqrt{8}}\sigma_2[\sigma_i S_j + \sigma_j S_i], \quad (2)$$

where S_i's are spin-$\frac{1}{2}$ to spin-$\frac{3}{2}$ transition matrices [8] and σ_i's are the usual Pauli matrices.

The interaction in Eq. (1) produces an s-wave amplitude; Fig. 1. It is a geometric series, summed to give

$$i\mathcal{A}^{(\kappa)}_{\mathrm{EFT}}(p) = \frac{ig^{(\kappa)}}{1 - ig^{(\kappa)}L(p)}, \quad (3)$$

where $g^{(\kappa)}$ corresponds to $g^{(1)}, g^{(2)}$ in the respective spin channels and $L(p) = -\frac{i\mu}{2\pi}(\lambda + ip)$ is the loop contribution with reduced mass μ at the renormalization scale λ. The loop integral $L(p)$ is evaluated in the power divergence subtraction scheme [15] where divergences in both $D=4$ and lower space-time dimensions are subtracted. Matching Eq. (3) to the low-energy effective range expansion (ERE) amplitude fixes the EFT couplings as

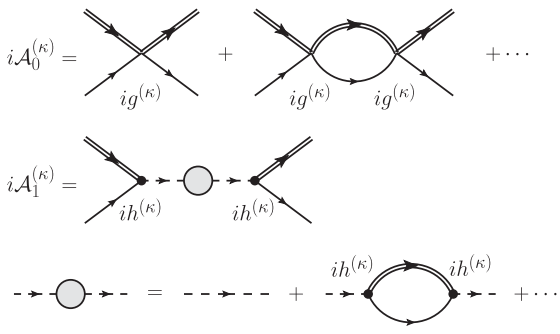

FIG. 1. $\mathcal{A}_0^{(\kappa)}$ is the $^3S_1, ^5S_2$ scattering amplitude. $\mathcal{A}_1^{(\kappa)}$ is the $^3P_2, ^5P_2$ scattering amplitude. Double line is the ^{7}Li propagator, single line the neutron propagator, dashed line the bare dimer propagator.

$g^{(\kappa)}(\lambda) = (2\pi)/[\mu(\lambda - 1/a_0^{(\kappa)})]$ with the scattering lengths $a_0^{(2)} = -3.63 \pm 0.05$ fm, $a_0^{(1)} = 0.87 \pm 0.07$ fm [16]. In Ref. [17], initial state interactions using ERE were also considered.

The final ^{8}Li bound state is in a p wave that we consider shallow similar to its isospin mirror ^{8}B nucleus. The EFT for shallow p-wave states was formulated in Ref. [8] where it was shown that, unlike s wave, it requires not one but two nonperturbative EFT interactions. The renormalization of loops is easily accomplished in the dimer formalism. The interactions in the $^3P_2$ and $^5P_2$ states are constructed by combining the matrices F_i, Q_{ij} and the Galilean invariant velocity difference vector $(\boldsymbol{v}_C - \boldsymbol{v}_N)_k$ into a p-wave dimer with total $J=2$. We write the p-wave Lagrangian as

$$\begin{aligned}\mathcal{L}^{(p)} = {} & \phi_{ij}^\dagger\left[\Delta^{(1)} + \left(i\partial_0 + \frac{\nabla^2}{2M}\right)\right]\phi_{ij} \\ & + \sqrt{3}h^{(1)}\left[\phi_{ij}^\dagger N^T F_x\left(\frac{\overrightarrow{\nabla}}{M_C} - \frac{\overleftarrow{\nabla}}{M_N}\right)_y C + \mathrm{H.c.}\right]R_{ijxy} \\ & + \pi_{ij}^\dagger\left[\Delta^{(2)} + \left(i\partial_0 + \frac{\nabla^2}{2M}\right)\right]\pi_{ij} + \frac{h^{(2)}}{\sqrt{2}} \\ & \times\left[\pi_{ij}^\dagger N^T Q_{xy}\left(\frac{\overrightarrow{\nabla}}{M_C} - \frac{\overleftarrow{\nabla}}{M_N}\right)_z C + \mathrm{H.c.}\right]T_{xyzij}, \end{aligned} \quad (4)$$

where ϕ_{ij} (π_{ij}) is the dimer in the $^3P_2$ ($^5P_2$) channel, and $R_{ijxy} = [\delta_{ix}\delta_{jy} + \delta_{iy}\delta_{jx} - \frac{2}{3}\delta_{ij}\delta_{xy}]/2$, $T_{xyzij} = [\epsilon_{xzi}\delta_{yj} + \epsilon_{xzj}\delta_{yi} + \epsilon_{yzi}\delta_{xj} + \epsilon_{yzj}\delta_{xi}]/2$. The interactions in $\mathcal{L}^{(p)}$ are equivalent to the ones with only neutron-core short-range interactions without a dimer field. In terms of Feynman diagrams, the four-fermion interaction is replaced in the dimer formulation by a dimer exchange; Fig. 1. The nonperturbative iteration of the leading operators is accomplished by ''dressing'' the dimer propagator with nucleon-core loops. For a given spin channel $\kappa = 1$ ($^3P_2$) or $\kappa = 2$ ($^5P_2$), the dressed dimer propagator, proportional to the elastic amplitude, reads

$$iD^{(\kappa)}(p_0, \boldsymbol{p}) = \frac{i}{\Delta^{(\kappa)} - \zeta^2/(2\mu) + 2h^{(\kappa)2}f(p_0, \boldsymbol{p})/\mu}, \quad (5)$$

where the loop contribution $f(p_0, \boldsymbol{p}) = \frac{1}{4\pi}(\zeta^3 - \frac{3}{2}\zeta^2\lambda + \frac{\pi}{2}\lambda^3)$ with $\zeta = \sqrt{-2\mu p_0 + \mu p^2/M - i0^+}$, $M = M_N + M_C$. Matching the EFT amplitudes to the p-wave ERE determines the coupling pair $(\Delta^{(\kappa)}, h^{(\kappa)})$. Again, only the first two ERE parameters are kept since EFT requires two operators at LO.

Radiative capture.—The LO capture cross section can be calculated via minimally coupling the photon by gauging the ^{7}Li core momentum $\boldsymbol{p}_C \to \boldsymbol{p}_C + Z_C e\boldsymbol{A}$, where $Z_C = 3$ is the ^{7}Li core charge. The $E1$ contribution comes from the diagrams in Fig. 2. The center-of-mass (c.m.) kinematics are defined with $\boldsymbol{p}$ ($\boldsymbol{k}$) the core (photon) momentum and $\hat{\boldsymbol{k}}\cdot\hat{\boldsymbol{p}} = \cos\theta$. Formally we take $p \sim \gamma$

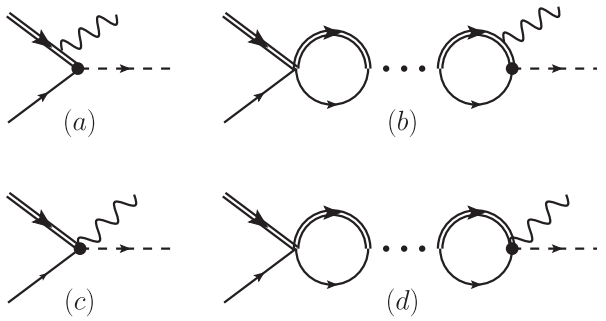

FIG. 2. ^{7}Li$(n,\gamma)^8$Li: Wavy lines represent photons. "…" represent initial state s-wave interaction.

as the small scale where $\gamma = \sqrt{2\mu B} \approx 57.8$ MeV, with $B \approx 2.03$ MeV the ^{8}Li binding energy. Then at LO the Mandelstam variable $s \approx (M_N + M_C)^2 = M^2$ and $|\boldsymbol{k}| = k_0 \approx (p^2 + \gamma^2)/(2\mu)$. We get for the c.m. differential cross section

$$\frac{d\sigma}{d\phi d\cos\theta} = \frac{1}{64\pi^2 s}\frac{|\boldsymbol{k}|}{|\boldsymbol{p}|}|\mathcal{M}|^2 \approx \frac{1}{64\pi^2 M^2}\frac{|\boldsymbol{k}|}{|\boldsymbol{p}|}|\mathcal{M}|^2. \quad (6)$$

The capture from the initial state $^5S_2$ to the $^5P_2$ final state (spin channel 2) dominates due to the larger initial state scattering length $a_0^{(2)} > a_0^{(1)}$. The divergence in Fig. 2(b) is canceled by Fig. 2(d) [9]. Summing over all polarizations and spins

$$|\mathcal{M}^{(^5P_2)}|^2 = 5\left(\frac{Z_C M_N}{M}\right)^2 \frac{64\pi\alpha M^2 |h^{(2)}\sqrt{\mathcal{Z}^{(2)}}|^2}{\mu} \times\left[|1+X|^2 - \frac{p^2\sin^2\theta}{p^2+\gamma^2}\left(\frac{2\gamma^2}{p^2+\gamma^2} + X + X^*\right)\right],$$
$$X = \frac{i}{-1/a_0^{(2)} - ip}\left(p - i\frac{2}{3}\frac{\gamma^3 - ip^3}{p^2+\gamma^2}\right), \quad (7)$$

with $\alpha = e^2/(4\pi)$, the dimer polarization sum $\sum \varepsilon_{ij}\varepsilon^*_{xy} = R_{ijxy}$ [18], and the wave function renormalization $|h^{(2)2}\mathcal{Z}^{(2)}| = 2\pi/|3\gamma + r_1^{(2)}|$, where $r_1^{(2)}$ is the effective range in the $^5P_2$ scattering amplitude. $\mathcal{Z}^{(2)}$ is defined as the residue at the pole in the dressed dimer propagator $D^{(2)}(p_0, \boldsymbol{p})$. The capture from $^3S_1$ to $^3P_2$ state has the same exact expression as Eq. (7) except that $a_0^{(2)}$, $r_1^{(2)}$, and $\mathcal{Z}^{(2)}$ are replaced by the corresponding parameters in the spin channel 1. The differential cross section averaged over initial spin states is

$$\frac{d\sigma}{d\cos\theta} = \frac{1}{32\pi M^2}\frac{|\boldsymbol{k}|}{|\boldsymbol{p}|}\frac{1}{8}\frac{|\mathcal{M}^{(^5P_2)}|^2 + |\mathcal{M}^{(^3P_2)}|^2}{2}, \quad (8)$$

taking the ^{8}Li nucleus as a symmetric combination $(|^3P_2\rangle + |^5P_2\rangle)/\sqrt{2}$ of final states.

The parameters in $\sigma(p)$ can be determined from elastic n-^{7}Li scattering data and ^{8}Li binding energy. However, the p-wave effective range $r_1^{(\kappa)}$ is not known accurately. This is the main theoretical uncertainty at this order. Changing the effective range $r_1^{(\kappa)}$ modifies $\mathcal{Z}^{(\kappa)}$ and moves the cross section up or down by a multiplicative factor. In traditional potential model calculations, the parameters are determined by reproducing the ^{8}Li binding energy. However, this does not constrain the effective range and other parameters of the ERE. For example, in a Woods-Saxon potential $V(r) = -v_0[1 + \exp(\frac{r-R_c}{a_c})]^{-1}$ different choices for the depth v_0, range R_c, diffusiveness a_c can be made to reproduce the known ^{8}Li binding energy. This, however, produces different effective ranges, and constitutes an irreducible source of error in the theoretical calculations.

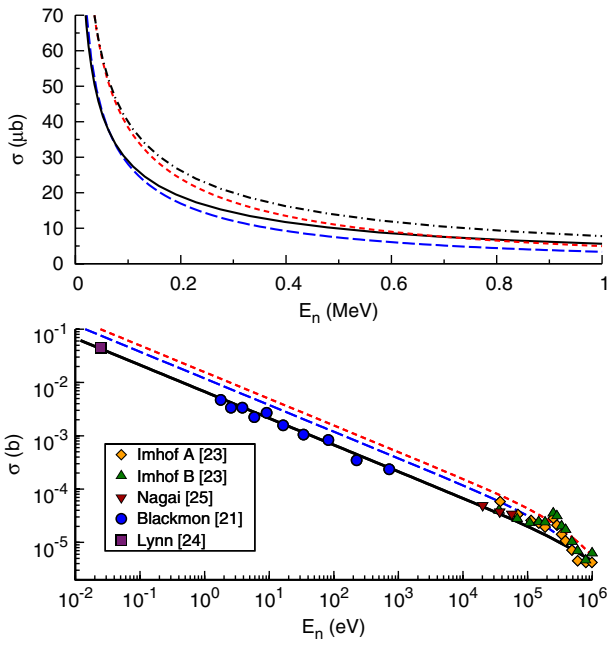

FIG. 3 (color online). Potential models: long-dashed blue curve from Davids-Typel [5], dashed red curve from Tombrello [12]. Top panel: solid black curve EFT with $r_1 = -0.3$/fm, dot-dashed black curve EFT with $r_1 = -0.46$/fm. Bottom panel: solid black curve EFT with r_1 fitted to data.

Comparing the contributions to the capture cross section from the two spin channels analytically, we get

$$\left.\frac{\sigma^{(^5P_2)}}{\sigma^{(^5P_2)} + \sigma^{(^3P_2)}}\right|_{p=0} = \left[1 + \frac{(3 - 2a_0^{(1)}\gamma)^2}{(3 - 2a_0^{(2)}\gamma)^2}\right]^{-1} \approx 0.81, \quad (9)$$

using the same effective range r_1 in both spin channels. This ratio is close to the experimentally observed ratio [19]. From Eqs. (7) and (8) one can see that the total cross section at low energy is not independently sensitive to $r_1^{(2)}$ and $r_1^{(1)}$. This is confirmed by our fit to data.

In Fig. 3, we compare potential model calculations using Tombrello's [12] and the Davids-Typel [5] parameters to EFT curves. At low energy the potential model results can be reproduced in EFT with a small variation in the effective

range $-0.46 \leq r_1 \leq -0.3$ fm^{-1}. At higher energies they differ since potential models include ERE parameters beyond the scattering length and effective range. A fit to data from Ref. [20] in the energy range $E_n \sim 2$–700 eV gives $r_1 = -1.47$ fm^{-1}. This value is compatible with the Wigner bound [21] which, for a nucleon-core interaction shorter than 3 fm, restricts r_1 to be smaller than around -1 fm^{-1}. Following Ref. [20], their data and the theory curves in the bottom panel in Fig. 3 were divided by the known experimental branching ratio 0.89 to the ground state and compared to a few other available data [22–24]. The r_1 was fitted to the unscaled data for transition to the ground state as appropriate. It is clear that the theory error at low energy comes from the uncertainty in the effective range at LO.

Conclusions.—Using a model-independent formalism we demonstrated and quantified the theoretical uncertainty in the ^{7}Li$(n, \gamma)^8$Li calculation associated with phenomenological potentials in the single-particle approximation. The LO result depends on the poorly known p-wave effective range parameter r_1. Without detailed knowledge about r_1, model calculations deviate from data at low energy. We extract this effective range parameter by fitting our analytic form to data.

We stress that this sensitivity to r_1 at low energies is a consequence of having two operators for shallow p-wave states at LO. Therefore, the conclusions of the present work also apply to the ^{7}Be$(p, \gamma)^8$B reaction. Coulomb interactions in $p + {}^7$Be scattering and ^{7}Be$(p, \gamma)^8$B reaction are under investigation [25].

The EFT expression for ^{7}Li$(n, \gamma)^8$Li capture is consistent with low-energy data, which is lower than model calculations [5,12] as shown. This reaction affects ^{7}Li abundances, and the impact of the uncertainty in r_1 in inhomogeneous BBN can be explored using our result.

At higher order in the EFT expansion, the cross section would get corrections from higher order initial and final state interactions and two-body currents. The former can be related to the ERE. At very low energy, it is the final state interactions, which modify the wave function renormalization constants, that are important. At next-to-next-to-leading order the shape parameter associated with p-wave interaction contributes [8,25]. In addition, at higher order two-body currents such as $E_i(NF_jC)^\dagger \times [NF_x(\overrightarrow{\nabla}/M_C - \overleftarrow{\nabla}/M_N)_y C]R_{ijxy}$, where E_i is the electric field, contribute. These operators are not constrained by elastic scattering. A higher order EFT calculation would reduce theoretical errors though at the expense of additional parameters. This is not a drawback as what we gain is a model-independent understanding of the sources of higher order contributions and a more detailed knowledge about the kind of experimental input that is required to better constrain the low-energy theory.

The authors thank P. Bedaque, C. Bertulani, B. Davids, V. Guimarães, C. Johnson, A. Mukhamedzhanov, S. Typel for valuable discussions; ECT*, INT, MSU (R. H.) for hospitality; and the HPCC center at MSU (G. R.), the U.S. NSF Grant No. PHY-0969378 (G. R.), the FOM programme 114 (R. H.), the BMBF Contract No. 06BN411 (R. H.) for partial support. Authors are extremely grateful to S. Typel for providing the potential model numbers.

*grupak@u.washington.edu
†R.Higa@rug.nl

[1] S. Burles, K. M. Nollett, J. W. Truran, and M. S. Turner, Phys. Rev. Lett. **82**, 4176 (1999).
[2] C. Rolfs and W. Rodney, *Cauldrons in the Cosmos* (University of Chicago Press, Chicago, 1988).
[3] S. W. Barwick *et al.*, arXiv:astro-ph/0412544.
[4] E. G. Adelberger *et al.*, Rev. Mod. Phys. **70**, 1265 (1998).
[5] B. Davids and S. Typel, Phys. Rev. C **68**, 045802 (2003).
[6] P. Descouvemont, Phys. Rev. C **70**, 065802 (2004).
[7] G. Rupak, Nucl. Phys. **A678**, 405 (2000).
[8] C. A. Bertulani, H. W. Hammer, and U. Van Kolck, Nucl. Phys. **A712**, 37 (2002); P. F. Bedaque, H. W. Hammer, and U. van Kolck, Phys. Lett. B **569**, 159 (2003).
[9] D. R. Phillips and H. W. Hammer, Eur. Phys. J. Web Conf. **3**, 06002 (2010).
[10] The Facility for Rare Isotope Beams (FRIB) at the Michigan State University, http://frib.msu.edu/.
[11] L. H. Kawano, W. A. Fowler, R. W. Kavanagh, and R. A. Malaney, Astrophys. J. **372**, 1 (1991).
[12] T. Tombrello, Nucl. Phys. **71**, 459 (1965).
[13] J. T. Huang, C. A. Bertulani, and V. Guimaraes, At. Data Nucl. Data Tables **96**, 824 (2010).
[14] L. Trache *et al.*, Phys. Rev. C **67**, 062801 (2003).
[15] D. B. Kaplan, M. J. Savage, and M. B.Wise, Phys. Lett. B **424**, 390 (1998); P. F. Bedaque and U. van Kolck, Phys. Lett. B **428**, 221 (1998); J.-W. Chen, G. Rupak, and M. J. Savage, Nucl. Phys. **A653**, 386 (1999).
[16] L. Koester, K. Knopf, and W. Waschkowski, Z. Phys. A **312** 81 (1983); C. Angulo *et al.*, Nucl. Phys. **A716**, 211 (2003).
[17] S. Typel and G. Baur, Nucl. Phys. **A759**, 247 (2005).
[18] S. Choi, J. Lee, J. S. Shim, and H. Song, J. Korean Phys. Soc. **25**, 576 (1992); S. Fleming, T. Mehen, and I. W. Stewart, Nucl. Phys. **A677**, 313 (2000).
[19] F. C. Barker, Nucl. Phys. **A588**, 693 (1995).
[20] J. C. Blackmon *et al.*, Phys. Rev. C **54**, 383 (1996).
[21] H. W. Hammer and D. Lee, Ann. Phys. (N.Y.) **325**, 2212 (2010).
[22] W. L. Imhof, R. G. Johnson, F. J. Vaughn, and M. Walt, Phys. Rev. **114**, 1037 (1959). The two data sets correspond to two different normalizations of the same data.
[23] J. E. Lynn, E. T. Jurney, and S. Raman, Phys. Rev. C **44**, 764 (1991).
[24] Y. Nagai *et al.*, Phys. Rev. C **71**, 055803 (2005).
[25] R. Higa and G. Rupak (to be published).